these conditions is quite negligible, the phenomenon probably arises from some modification of the nucleation mechanism itself. This cannot be occurring through the "temperature" of the pulse being above ambient because ν is found to be independent of i_0 although it remains possible, of course, that the nucleation process for an individual ion is perturbed by the bunch of rotons which it has itself created and whose density presumably increases with F. Our results would seem to favor models[14] in which the vortex ring is formed initially in a symmetrical position around the ion which, for small F, will subsequently move sideways and become trapped; and to weigh against models[15] in which a vortex loop is gradually paid out from the ion, which is therefore always trapped.

†Work supported by the Science Research Council under Contract No. BRG6094.8.

[1]L. D. Landau, *Introduction to the Theory of Superfluidity*, translated by I. M. Khalatnikov (Benjamin, New York, 1965).

[2]G. W. Rayfield, Phys. Rev. Lett. 16, 934 (1966), and Phys. Rev. 168, 222 (1968).

[3]E. H. Takken, Phys. Rev. A 1, 1220 (1970).

[4]D. A. Neeper, Phys. Rev. Lett. 21, 274 (1968); D. A. Neeper and L. Meyer, Phys. Rev. 182, 8223 (1969).

[5]A. Phillips and P. V. E. McClintock, Phys. Lett. 46A, 109 (1973).

[6]A. Phillips and P. V. E. McClintock, J. Phys. C: Proc. Phys. Soc., London 7, L118 (1974).

[7]For a discussion of pulse shapes, see K. W. Schwarz, Phys. Rev. A 6, 837 (1972).

[8]R. J. Donnelly, Phys. Lett. 39A, 221 (1972).

[9]R. J. Donnelly, *Experimental Superfluidity* (Univ. of Chicago Press, Chicago, Ill., 1967).

[10]B. E. Springett and R. J. Donnelly, Phys. Rev. Lett. 17, 364 (1966).

[11]J. Poitrenaud and F. I. B. Williams, Phys. Rev. Lett. 29, 1230 (1972), and 32, 1213 (1974).

[12]A. Phillips and P. V. E. McClintock, to be published.

[13]C.f. measurements of ν for small F by J. A. Titus and J. S. Rosenshein, Phys. Rev. Lett. 31, 146 (1973); and R. Zoll and K. W. Schwarz, Phys. Rev. Lett. 31, 1440 (1973): These investigations found ν to increase monotonically with F, although the latter authors inferred from their high-pressure data for $F \leq 25$ V cm^{-1} that $\nu(F)$ was approaching an asymptotic limit in large fields.

[14]K. W. Schwarz and P. S. Jang, Phys. Rev. A 8, 3199 (1973).

[15]R. J. Donnelly and P. H. Roberts, Phil. Trans. Roy. Soc. London, Ser. A 271, 41 (1971).

Focused-Flow Model of Relativistic Diodes*

S. A. Goldstein and R. C. Davidson
University of Maryland, College Park, Maryland 29742

and

J. G. Siambis and Roswell Lee
Naval Research Laboratory, Washington, D.C. 20375

(Received 29 August 1974)

A new model of electron flow in high-voltage diodes and superpinch formation is presented. The relativistic cold-fluid–Maxwell equations are reduced, under certain assumptions, to one equation. The model is based on the solution for the electron flow in large aspect-ratio diodes and the inclusion of cathode and anode plasmas. The anode plasma is assumed to be a field-free region. Results are compared to the parapotential-flow model.

The behavior of relativistic electron flow inside high-voltage (~1 MV) diodes is important for obtaining extremely high current densities[1-3] and for applications to controlled thermonuclear fusion experiments.[4] The strong pinching observed experimentally[1-3] on the anode surface has motivated the theoretical investigation and modeling of the so-called superpinch. The parapotential-flow model[5,6] predicts scaling laws of diode impedance but is unable to treat electron flow near the cathode or the anode. The metapotential-flow model[1] contains the effects of orbit crossings but relies sensitively on anode plasma dynamics and/or strong plasma bias currents for superpinch formation.

In the focused-flow model presented in this work we treat the electrons within the framework of the steady-state ($\partial/\partial t = 0$) relativistic-fluid–

Maxwell equations. We assume that the flow is cold (pressureless) and the electron beam is fully nonneutral. The equations are reduced to one second-order partial differential equation for the electron momentum in the limit that the energy is constant, not only along current flow lines, but also constant across current flow lines in the diode region. The treatment is fully self-consistent and includes the influence of self-field effects on the relativistic electron flow. The equations describing steady-state flow are given by

$$\nabla\cdot(n\vec{u})=0, \tag{1}$$

$$\vec{u}\cdot\nabla\vec{p}=e(\vec{E}+\vec{u}\times\vec{B}/c), \tag{2}$$

$$\nabla\cdot\vec{E}=4\pi en, \quad \vec{E}=-\nabla\varphi, \tag{3}$$

$$\nabla\cdot\vec{B}=0, \quad \nabla\times\vec{B}=4\pi\vec{J}/c=4\pi en\vec{u}/c, \tag{4}$$

$$\vec{p}=m\vec{u}, \quad m=m_0/[1-(u/c)^2]^{1/2}, \quad \gamma^2=1+p^2/m_0^2c^2, \tag{5}$$

where n is the electron density, $\vec{u}$ is the mean velocity of an electron fluid element, $\vec{E}$ and $\vec{B}$ are the electromagnetic fields, c is the speed of light *in vacuo*, m_0 and e are the electron rest mass and charge, respectively, and cgs electrostatic units are used throughout the present analysis. The energy constant of the motion implied by Eqs. (1)–(4) is given by

$$\vec{J}\cdot\nabla[e\varphi+(\gamma-1)m_0c^2]=0, \tag{6}$$

and reduces to the form $e\varphi+(\gamma-1)m_0c^2=\text{const}$ in the present analysis. From Eqs. (2), (3), (5), and (6) and the vector identity, $\nabla(G^2/2)=\vec{G}\times(\nabla\times\vec{G})+(\vec{G}\cdot\nabla)\vec{G}$, it follows that $\vec{p}\times(\nabla\times\vec{p}+e\vec{B}/c)=0$ For azimuthal symmetry ($\partial/\partial\theta=0$) and no θ rotation, we find

$$\nabla\times\vec{p}=-e\vec{B}/c. \tag{7}$$

Combining Eqs. (3)–(7), it is straightforward to show that

$$\nabla\times(\nabla\times\vec{p})=-\vec{p}(\nabla^2\gamma)/\gamma. \tag{8}$$

Equation (8) and the boundary conditions on $\vec{p}$ and the electromagnetic fields constitute the basic equations to be solved.

Equation (8) is solved by means of an asymptotic expansion in the limit of small inverse aspect ratio $\epsilon=D_0/R_0\ll1$, where D_0 is the gap spacing between anode and cathode plasmas, and R_0 is the cathode radius of the planar, azimuthally symmetric diode (Fig. 1). Anode and cathode plasma layers are assumed present as illustrated in Fig. 1. The gap is divided into five regions

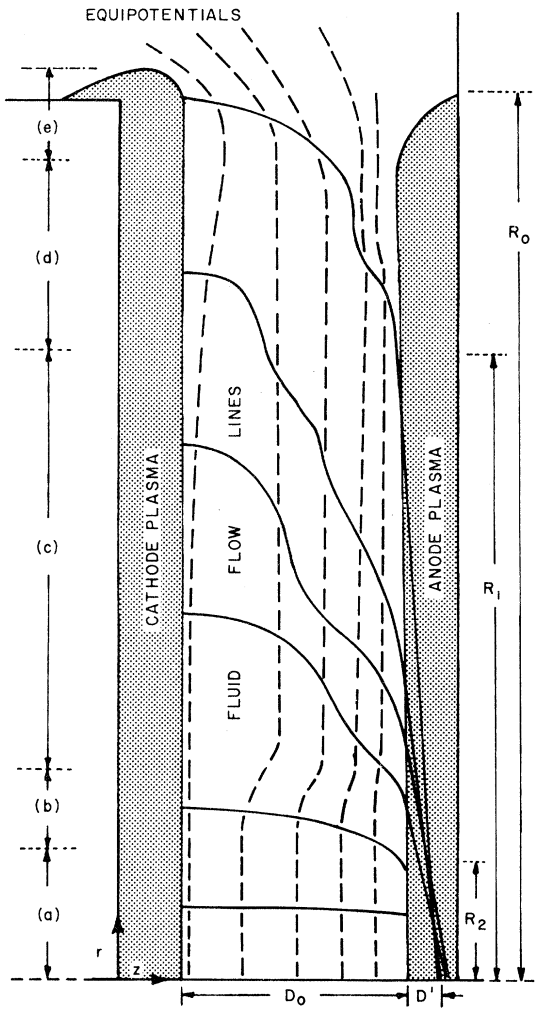

FIG. 1. Diode geometry with computed equipotentials and fluid flow lines.

and solutions are obtained from Eq. (8), for regions (a), (c), and (d). Shank emission is neglected in the present analysis because it is suppressed by the high magnetic fields. Equation (8) can be expressed in explicit form as

$$\frac{1}{r}\frac{\partial}{\partial r}r\left(\frac{\partial q_r}{\partial z}+\frac{\partial q_z}{\partial r}\right)=q_z\frac{1}{\gamma}\nabla^2\gamma, \tag{9}$$

$$\frac{\partial}{\partial z}\left(\frac{\partial q_r}{\partial z}+\frac{\partial q_z}{\partial r}\right)=q_r\frac{1}{\gamma}\nabla^2\gamma, \tag{10}$$

where z and r denote the dimensionless variables z/D_0 and r/D_0, and

$$q_z=p_z/m_0c, \quad q_r=-p_r/m_0c. \tag{11}$$

We solve Eqs. (9) and (10) subject to the assumptions $\gamma\simeq\gamma(z)$, and $\vec{E}=0$ on the cathode-plasma

surface, and make use of the boundary conditions $\gamma(z=0)=1$ and $\gamma(z=1)=1-eV_0/m_0c^2\equiv\gamma_0$, where V_0 is the diode voltage. For $\gamma_0<3$, the approximate solutions for q_r and q_z in region (a) are given by

$$q_r=krz,$$
$$q_z^2=[1+(\gamma_0-1)z^{4/3}]^2-1-(krz)^2, \tag{12}$$

where $k=\frac{8}{9}[(\gamma_0-1)/2)]^{3/2}$. Further iterations can generate better approximations to the exact solution. The radius R_2 (Fig. 1) is defined by the relation $q_z^2(z=1)=q_r^2(z=1)$, which gives

$$R_2=(\gamma_0+1)^{1/2}[9D_0/4(\gamma_0-1)]\approx 2D_0 \tag{13}$$

for $\gamma_0=3$. The magnetic field at R_2 obtained from Eqs. (7) and (12) is

$$B_\theta=\frac{m_0c^2}{eD_0}\left(\frac{\gamma_0^2-1}{2}\right)^{1/2}. \tag{14}$$

In region (b) none of the terms in Eqs. (9) and (10) may be neglected, and strong radial electric fields and $q_r\sim q_z$ characterize the flow. No analytical solution has been obtained in this region.

In region (c), Eq. (8) can be expressed as

$$\epsilon\frac{1}{r}\frac{\partial}{\partial r}r\left(\frac{\partial q_r}{\partial z}+\epsilon\frac{\partial q_z}{\partial r}\right)=\frac{q_z}{\gamma}\frac{\partial^2\gamma}{\partial z^2}, \tag{15}$$

$$\frac{\partial}{\partial z}\left(\frac{\partial q_r}{\partial z}+\epsilon\frac{\partial q_z}{\partial r}\right)=\frac{q_r}{\gamma}\frac{\partial^2\gamma}{\partial z^2}, \tag{16}$$

where r and z are now normalized to R_0 and D_0, respectively, and terms of order ϵ^3 have been neglected in the term $\nabla^2\gamma$. Inspection of Eqs. (15) and (16) reveals that $q_z\sim\epsilon$ for all z, and that q_r is of order unity near the anode but approaches zero faster than q_z near the cathode. An iterative flip-flop procedure is used to solve Eqs. (15) and (16). [In particular, we solve Eq. (16) for q_r assuming $q_z=0$. The resulting expression for q_r is then used in Eq. (15) to solve for q_z. We then return to Eq. (16) and iterate.] The result for q_r, correct to order ϵ^2, is given by

$$q_r=\tfrac{1}{2}[\exp(c_0z)-\exp(-c_0z)], \tag{17}$$
$$c_0=\ln[\gamma_0+(\gamma_0^2-1)^{1/2}]. \tag{18}$$

The solution for q_z is an oscillatory function (Fig. 2) and its first half-oscillation, near the cathode, can be expressed as

$$\arcsin(q_z/A)^{1/2}-[(q_z/A)(1-q_z/A)]^{1/2}=c_0z/A, \tag{19}$$

where $A=2\epsilon/rc_0$. For $z\ll 1$ and $q_z/A\ll 1$, we find $q_z=(9\epsilon c_0/2r)^{1/3}z^{2/3}$, which is reminiscent of

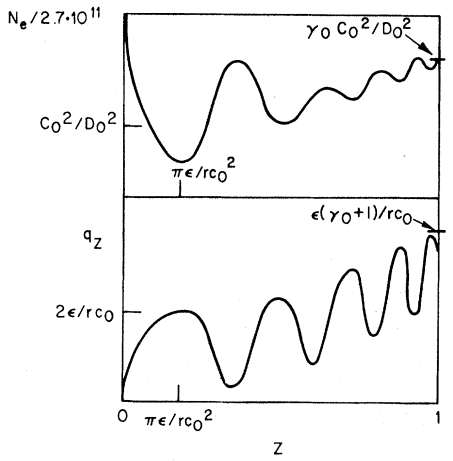

FIG. 2. Sketch of density n and axial momentum q_z versus z, in region (c).

Child-Langmuir space-charge-limited flow. The current density, however, varies as $1/r$ as opposed to a constant for cases where the Child-Langmuir law applies in the entire diode region. The solution for q_z in regions further away from the cathode is more complicated, and the essential elements of the flow are illustrated qualitatively in Fig. 2. The mathematical form of q_z will be treated elsewhere.[7]

In region (c) the magnetic field is found to be

$$B_\theta=-(c/e)(\nabla\times\vec{p})_\theta$$
$$=(m_0c^2/2eD_0)c_0[\exp(c_0z)+\exp(-c_0z)]. \tag{20}$$

The expressions for B_θ given in Eq. (20) [region (c)] and Eq. (14) [region (a)] are comparable in magnitude, which facilitates matching of solutions in region (b). An approximate solution for region (d) has also been obtained, but will be presented elsewhere.[7] The solution for the flow in region (e) has to be matched to vacuum field solutions that contain strong radial electric fields. No attempt has been made to solve Eq. (8) near the cathode corner. Only approximate equipotentials are used.

The overall picture of the electron flow in the gap, as found from the analytical solutions in the various regions, is illustrated in Fig. 1. There it is seen that equipotential surfaces remain nearly vertical and are not conic as assumed in the parapotential-flow theory. At larger radii, the electron-fluid flow lines have a large component of velocity along equipotential surfaces and a smaller component across equipotentials. To lowest order in ϵ, this motion is an $\vec{E}\times\vec{B}$ drift as

in the parapotential flow model. The pinching observed in the vacuum region of the diode is weak. In particular, for region (c) the radial location of the flow at the anode-plasma surface is $r_A=(1/\gamma_0)r_c$, where r_c is the radial location of the same current flow line at the cathode-plasma surface. The current flow lines, however, graze the surface of the anode plasma at very small angles. Assuming charge and current neutralization for the relativistic electrons inside the anode plasma, the electrons flow free after entering the anode plasma and focus on the z axis of the diode. The effective focal length, measured from the vacuum–anode-plasma interface, is found to be

$$D' \simeq D_0\gamma_0(\gamma_0^2-1)^{-1/2}\{\ln[\gamma_0+(\gamma_0^2-1)^{1/2}]\}^{-1} \quad (21)$$

with an axial dispersion of order D'/γ_0. The closure of anode and cathode plasmas in region (c) is retarded by magnetic field pressure for times less than the classical diffusion time into a conducting plasma, $\tau_B \sim 2\times10^{-12}l^2T^{3/2}/z\ln\Lambda$. For example, if $l=0.1$ cm, $T=10^5$ °K, $z=1$, $\ln\Lambda=10$, then $\tau_B \sim 60$ nsec which is comparable to experimental times of interest.[3]

The total current, calculated from Eqs. (4) and (20) at radius R_1 of the outermost electron flow at the anode-plasma surface, is (in amperes)

$$I=8500(R_1/D_0)\gamma_0\ln[\gamma_0+(\gamma_0^2-1)^{1/2}], \quad (22)$$

where R_1 is estimated to be $R_1 \sim R_0/\gamma_0^{1/2}$. The current given in Eq. (22) is smaller by a factor $\gamma_0^{1/2}$ than the current obtained from the parapotential-flow model[6]; this result is in reasonable agreement with the data represented by Parker[8] and with recent measurements by Cooperstein, Condon, and Boller[3] that correct D_0 for gap closure.

The focused-flow model of beam formation and pinching in relativistic diodes, presented for the first time in this Letter, offers a new model of relativistic diode dynamics, that treats the electron flow from cathode to anode in a fully self-consistent manner including all self-field effects. The basic equation [Eq. (8)] may be used to describe the laminar flow of an unneutralized electron beam in a variety of circumstances [e.g., diodes, drift tubes, etc.].

The authors wish to thank Dr. John Guillory and Dr. Gery Cooperstein for helpful discussions.

*Research supported in part by the U.S. Office of Naval Research. The research of one of the authors (R. C. D.) was supported in part by the National Science Foundation.

[1]G. Yonas, K. R. Prestwich, J. W. Poukey, and J. R. Freeman, Phys. Rev. Lett. 30, 164 (1973).

[2]W. C. Condit, Jr., D. O. Trimble, G. A. Metzger, D. G. Pellinen, S. Heurlin, and P. Creely, Phys. Rev. Lett. 30, 123 (1973).

[3]G. Cooperstein, J. J. Condon, and R. J. Boller, Bull. Amer. Phys. Soc. 18, 1310 (1973), and to be published.

[4]F. Winterberg, Phys. Rev. 174, 212 (1968).

[5]D. C. dePackh, Naval Research Laboratory Internal Report No. 5, 1968 (unpublished).

[6]J. Creedon, Physics International Report No. PIIR-17-72, 1972 (to be published).

[7]S. A. Goldstein, R. C. Davidson, J. G. Siambis, and R. E. Lee, to be published.

[8]R. K. Parker, Ph.D. thesis, Nuclear Engineering Department, The University of New Mexico, 1973 (unpublished), Figs. 8–10.

Pressure-Dependent Electronic Transport in Amorphous As_2Se_3

G. Pfister
Xerox Webster Research Center, Webster, New York 14580
(Received 4 September 1974)

Room-temperature pressure studies (<3 kbar) on a-As_2Se_3 reveal that both hole transport, as determined from time-of-flight experiments, and dark dc conductivity increase with hydrostatic pressure as $\exp(\alpha p)$, where $\alpha \sim 0.45$ kbar^{-1}, independent of sample parameters. The pressure dependence and the shape of the phototransient strongly support the recently proposed stochastic hopping transport. The pressure dependence of the dark conductivity suggests a bulk controlled process.

The mechanisms of electronic transport in amorphous solids are of considerable current interest. The frequency dependence of the ac conductivity $\sigma(\omega)$,[1] and the dispersive photocurrent transient $I(t)$ observed in time-of-flight experiments,[2-4] indicate that, besides conventional band-type conduction, carrier transport may be occurring via phonon-assisted hopping among lo-